Building Simulation

Seventh International IBPSA Conference
Rio de Janeiro, Brazil
August 13-15, 2001

SIMULATING THE OPERATION OF PHOTOSENSOR-BASED LIGHTING CONTROLS

Charles Ehrlich, Konstantinos Papamichael, Judy Lai, and Kenneth Revzan

Building Technologies Department
Environmental Energy Technologies Division
Ernest Orlando Lawrence Berkeley National Laboratory
1 Cyclotron Road
Berkeley CA 94720 USA

ABSTRACT

Energy savings from the use of daylighting in commercial buildings are realized through implementation of photoelectric lighting controls that dim electric lights when sufficient daylight is available to provide adequate workplane illumination. The dimming level of electric lighting is based on the signal of a photosensor. Current simulation approaches for such systems are based on the questionable assumption that the signal of the photosensor is proportional to the task illuminance. This paper presents a method that simulates the performance of photosensor controls considering the acceptance angle, angular sensitivity, placement of the photosensor within a space, and color correction filter. The method is based on the multiplication of two fisheye images: one generated from the angular sensitivity of the photosensor and the other from a 180- or 360-degree fisheye image of the space as "seen" by the photosensor. The paper includes a detailed description of the method and its implementation, example applications, and validation results based on comparison with measurements in an actual office space.

INTRODUCTION

Controlling the output of electric lights using photosensor-based control technology can maximize energy savings resulting from daylighting while preserving occupant comfort and productivity [Rubinstein, 1984]. Predicting the performance of the electric lighting control system and its effects on energy use and other building performance parameters requires accurate daylighting and electric lighting simulation and reliable simulation of the photosensor's behavior in response to the variable physical conditions in which it is installed [Mistrick, et al., 1997]. Whole building simulation programs make simplifying assumptions for both of these simulations that reduce the overall accuracy of the calculations of the energy saved by daylighting. In addition, successful installation and operation of photo-sensor-based controls has proven difficult and expensive because it requires on-site experimentation under a variety of daylighting conditions.

This paper describes a simulation method that considers the geometric and material conditions of a room and the angular sensitivity, color correction filter, and placement of the specific photosensor device used. This method is demonstrated to accurately predict the photosensor signal strength of an actual photosensor-controlled lighting system installed at the Oakland Federal Building [Lee, et al., 1998]. The method can be used to assist with the design of photosensor-based controls as well as their installation, calibration, and operation.

The paper includes a detailed description of the simulation method and its implementation as well as its validation based on comparison with measured data in an actual office space. This simulation method can be used to predict the performance of photosensor-based controls in whole building simulation programs, which will improve our understanding of the operation of the control system and the accuracy of estimations of the energy it will save. Furthermore, our method can be used to pre-calibrate a specific proposed photosensor-controlled lighting system in a virtual office space and to determine how effectively the system will operate.

BACKGROUND

Typical photosensor-based electric lighting control systems for commercial offices include a photosensor strategically mounted either on the ceiling or under the luminaire close to the daylight aperture (see Figure 1). A typical photosensor is a silicon photodiode equipped with a diffuser that integrates the luminance of the surrounding surfaces. Some photosensors have a hemispherical view of the room whereas others have a view that extends beyond the hemisphere. More importantly, the sensitivity to light within the cone of view varies dramatically (see Figure 2) with some sensors being highly sensitive within a very narrow angle and others having a non-symmetrical sensitivity.

Silicon photodiodes are sensitive to a different band of the electromagnetic spectrum than the human eye;

their sensitivity extends into the UV and IR ranges. Therefore, photosensors are usually equipped with a color correction filter to approximate the human eye's response to light. A variety of simple electrical control circuits adjust the photosensor output signal voltage [Rubinstein, 1984]. The photosensor circuitry is connected to the lighting control system, which dims the electric lights when adequate daylight is available, and increases electric lighting when daylight availability drops, in order to maintain adequate workplane illuminance levels. Problems with the design, simulation, and calibration of such systems arise when it is assumed that the photosensor signal is a reliable measure of workplane illuminance. In fact, the photosensor response is a function of the luminance distribution of the surfaces seen by the sensor.

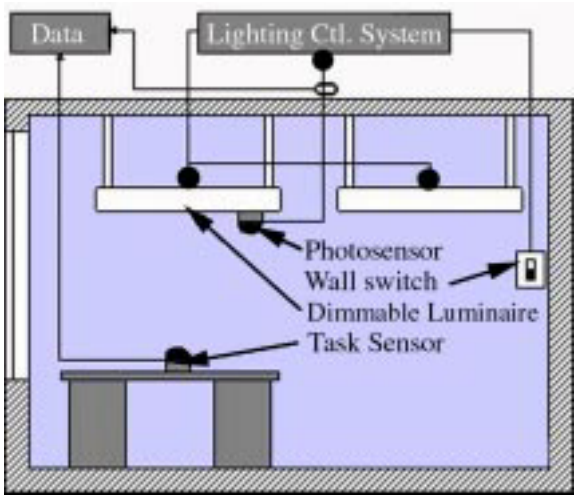

Figure 1. Schematic diagram of a typical installation of photosensor-based controls in a commercial office. Lines indicate power or data connections between components. Dashed arrows indicate connections and components needed only for collecting performance data.

Photosensor controls often do not work as expected and, as a result, room occupants often do not accept them [Love, 1995; Mistrick, 2000]. One of the reasons that they do not work is that we do not simulate their actual performance during design and then end up having to make them work at the site after installation.

Current simulation approaches [Choi, et al., 1997; Clark, et al., 1998; Winkelmann, 1983] to photosensor performance prediction make several simplifying assumptions that compromise the accuracy of predictions. Whole-building simulation programs, such as DOE-2, operate on the assumption that the photosensor signal is proportional to the daylight illuminance at a selected reference point. The photosensor placement and its angular and spectral response are not accounted for. In addition, most daylighting simulation approaches cannot model complex room geometry and the effects of partitions and furniture. However, photosensor performance is dependent upon all of these factors [Rubinstein, 1984; Rubinstein et al., 1989]. Researchers are attempting to improve the accuracy and reliability of photosensor performance simulation. An early version of a photosensor simulation program called DAYDIM and developed by Mistrick et al. considers the limitations of the specific photosensor control algorithm.

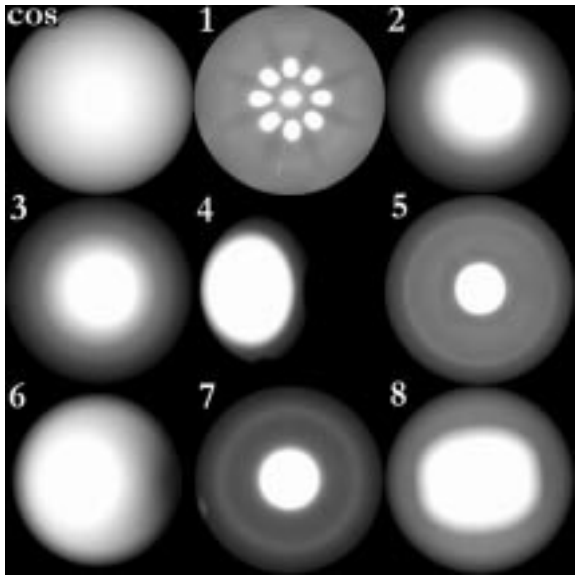

Figure 2. An ideal cosine spatial sensitivity distribution plus the eight photosensor distributions of Bierman and Conway, shown here as fisheye images.

Research performed by Bierman and Conway [Bierman, et al., 2000] demonstrates that different photosensor models have different acceptance angles and widely varying spatial and spectral sensitivities. The color-correction filter used with most sensors does not adequately approximate the photometric curve. Photosensor behavior can vary widely depending upon the sensor's placement in the room, the room surface reflectance, the placement of furniture, and the sensor's view of brightly lit exterior surfaces.

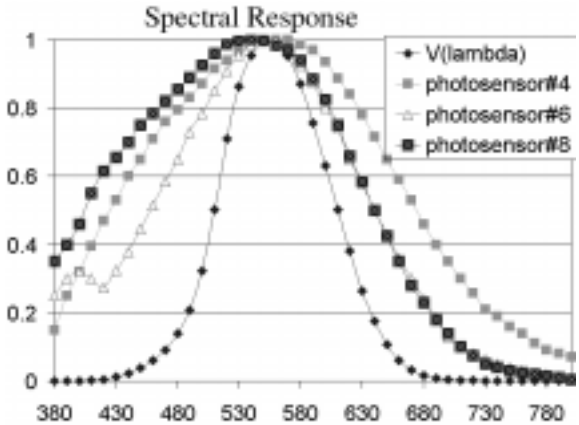

Figure 3. Three representative photometric correction filters and the CIE 1924 V-lambda photometric curve, an ideal color correction used to convert spectral radiance to illuminance.

The Bierman and Conway study provides the data necessary to improve the accuracy of simulations of the actual performance of photosensors. The varied angular responses of the eight photosensors considered in their study are shown in Figure 2 along with a theoretical cosine-corrected photosensor distribution. These data are provided in a two-dimensional file containing the relative sensor signal strength at each altitude and azimuth orientation.

The spectral response of these photosensors also varies. Figure 3 shows three spectral curves that represent the eight photosensors of the Bierman and Conway study plotted against the Commission International de l'Eclairage (CIE) 1924 V-lambda photometric curve. These data are stored in a standard ASCII file with the first column containing wavelength in nanometers and the second column containing the transmittance.

Figure 4. This 180-degree fisheye image shows the model of the room used for validation of the simulation method from the perspective of a photosensor mounted under the pendant luminaire. Notice the windows on the right side showing brightly illuminated exterior surfaces.

SIMULATION METHOD

A new simulation method has been devised based on the notion that the view of a photosensor and its angular sensitivity data can be represented by fisheye images (see Figure 2). The fisheye projection maps points that are 180 degrees from the nadir to a circle equidistant from the center of the image. Where the photosensor is more sensitive to light, the fisheye image will be whiter (corresponding to larger values) and where it is less sensitive, it will be blacker (corresponding to smaller values). Furthermore, the particular view of the room as "seen" by the photosensor can also be represented by a color, fisheye image (Figure 4). The predicted photosensor signal is idealized as the pixel-by-pixel multiplication of these two fisheye images, one generated from the angular acceptance curve of the control photosensor and the other from a 180- or 360-degree fisheye *Radiance* [Ward, et al., 1989] simulation of the space as "seen" by the photosensor. The sum of the pixel values of the new fisheye image, adjusted by the photosensor's spectral response, corresponds to the signal of the photosensor and can be converted to the actual output voltage by multiplication with an appropriate scaling factor.

This method requires that the scene be accurately modeled in three dimensions, including interior as well as exterior surface conditions. The image-generation process must accurately account for the interaction of light with all surfaces and materials and must accurately represent the luminance of the sky dome and solar disk. Although a variety of simulation programs offer many of these capabilities, only *Radiance* offers an accurate representation of the sky-dome luminance (when viewed directly) and can generate fisheye images. *Radiance's* daylighting prediction accuracy has been extensively validated by independent researchers [Khodulev, et al., 1996; Mardaljevic, 1995].

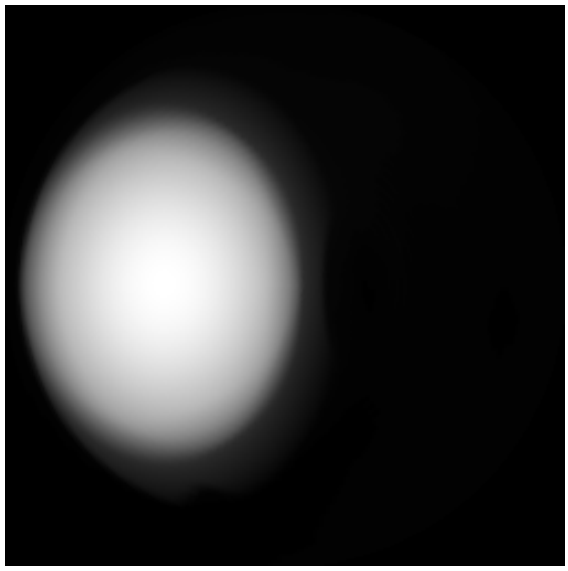

Figure 5. An example photosensor sensitivity fisheye image showing a strong lateral bias. This type of photosensor is often used next to windows to reduce the effect of bright exterior surfaces on the photosensor signal.

The image file format is another important feature of *Radiance* because each pixel represents a three-point spectral sample (red, green, and blue, RGB) in watts per steradian per square meter (radiance). In other words, the pixel values have not been flattened into a 8-bit, integer color space nor converted to luminance using an arbitrary photometric curve. The implementation and use of the simulation method is described step by step below.

The first step is to generate a fisheye representation of the angular sensitivity of the photosensor. A new *Radiance* program called **mksens** converts photosensor data into an RGB image. This image can then be viewed to determine the spatial orientation of the photosensor (Figure 2). To run the program, use the following syntax:

```
mksens [-r resolution]
"sensitivity file" >
"radiance image"
```

where resolution refers to the resolution of the output image in pixels.

Figure 5 shows the sensitivity image of a photosensor with a strong lateral bias. If this sensor's intended use will direct its more sensitive side toward the back of the room, then the appropriate rotation of the data can be determined. The photosensor in Figure 5 is appropriately oriented for placement in the room shown in Figure 4, so no rotation of the spatial sensitivity data is necessary. The photosensor angular sensitivity data is a standard ASCII file with two-dimensional data provided in two-degree increments. The first line is a header listing the azimuth angle values. Each line thereafter starts by listing the specific elevation angle and iterates through the azimuth angles, providing the measured response of the photosensor.

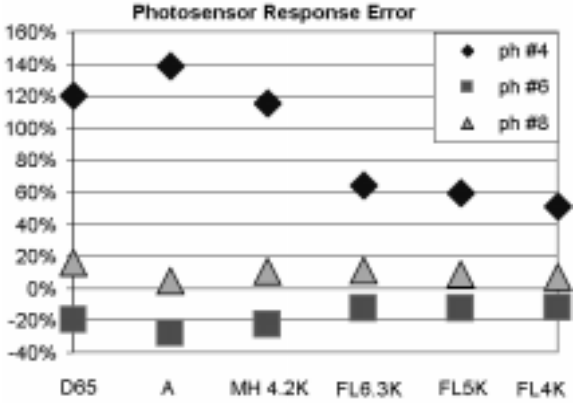

Figure 6. Relative error of three representative spectral curves illuminated by daylight (D65), incandescent (A), 4200K Metal Halide (MH 4.2K), 6300K fluorescent (FL6.3K), 5000K fluorescent (FL5K), and 4000K fluorescent (FL4K).

The second step in the simulation process is to model the scene geometry. The model may be of any degree of complexity, and it should include furniture and appropriate glazing specifications. Achromatic material specifications can be used if strong colors are not likely to be present in the room; however, this may introduce some error because of the photometric calibration of the photosensors. Extra care should be taken to model nearby exterior geometry, such as the ground surface or neighboring buildings, because the brightness of these surfaces can be hundreds of times greater than the brightness of the interior surfaces. Even if the photosensor "sees" only a small fraction of a brightly lit exterior surface, this can greatly affect its response.

The third step in the simulation method is to compute a fisheye image of the space from the location and in the view direction of the photosensor, as shown in Figure 4. If the photosensor acceptance angle extends beyond a hemisphere, then a 360-degree fisheye must be rendered.

The forth step is to convert the photometric correction filter spectral data file into a *Radiance* red, green, blue approximation. The Radiance RGB color specification format represents a three-point sampling of the visible spectrum. As shown in Figure 3, the three representative calibration filters do not accurately estimate the V-lambda curve. Most important, the error varies significantly (depending upon photosensor model) for different sources (see Figure 6), which is difficult to account for in the lighting control algorithm. This means that some photosensors will respond differently to different combinations of daylight and electric light. The spectral data must be converted into the RGB format to allow **psens** to compensate for the varying spectral selectivity of different photosensors. (This conversion process is described in detail in *Rendering with Radiance)* [Ward, et al., 1999]. The resulting values are specified on the command-line using the -R, -G, and -B options. If no color correction factor is specified, **psens** uses the default values of 0.265074126, 0.670114631, 0.064811243 for red, green, and blue respectively, approximating the standard photometric curve.

The final step is to compute the product of the photosensor sensitivity and room fisheye images using the newly developed program **psens**. For computational efficiency, this program does not actually multiply each image pixel by pixel; instead, it refers directly to the sensitivity data file while computing the resulting image. The program constructs a lookup table, mapping altitude and azimuth for each pixel in the image file. This lookup table is used to find the sensitivity. It then computes the approximate solid angle represented by the pixel to determine the appropriate area weighting of the pixel value. For computational efficiency, the program assumes that the projected shape of each pixel is a square. In fact, the shape is closer to a trapezoid and varies in orientation and form across the image. However, as described in the validation section below, this assumption seems to be a valid approximation. The program then multiplies the image pixel value, sensitivity factor, and solid angle weight to give the final result. The sum of all of these interpolated pixel values is multiplied by the color correction factor specified as a red, green, blue triplet on the command line to provide the final result. Equation 1 explains the relationship between

total photosensor response and the input parameters. The commands to execute this last step are:

```
psens -s "sensitivity file" [-r
rotation] [-R redSens -G grnSens
-B bluSens] "radiance image"
```

where rotation is the number of degrees to rotate the spatial sensitivity data to align the sensor with the desired orientation relative to the room fisheye image. The output results show the following:

```
Total solid angle: 7.45591
Total sensitivity: 2.20607
Response: 48.0008
```

where the total solid angle is the spatial extent of the sensitivity data (in steradians), total sensitivity is the sum of the sensitivity factors as found in the input file, and response is the predicted photosensor signal strength.

$$R = \sum \left[B_R S_R(\theta,\phi) P_R(\theta,\phi) B_G S_G(\theta,\phi) P_G(\theta,\phi) + B_B S_B(\theta,\phi) P_B(\theta,\phi) \right] \Omega(\theta,\phi)$$

Equation 1. The equation for total photosensor response, R, where B is brightness coefficient, S is photosensor sensitivity, P is pixel value, and Ω is the solid angle subtended by the square surrounding the pixel. The suffix indicated the color and each pixel is represented by its spherical coordinates, Φand Φ.

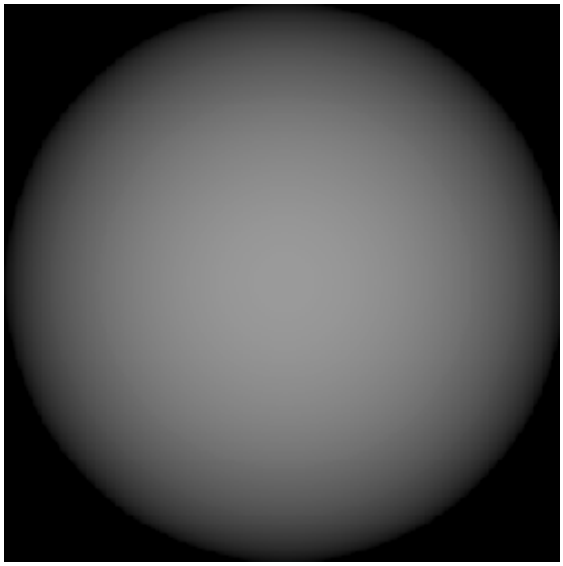

Figure 7. This image shows the ideal, cosine-corrected photosensor sensitivity distribution. The sum of the pixel brightness of this image is 1.0; it was used to validate the angular summation code.

VALIDATION

The authors validated their simulation method both by using hypothetical data to verify the code and by using actual data collected from an office installation at the Oakland Federal Building. Code validation involved comparing the output from **psens** with a known data set to verify that the pixel area weighting assumptions provide accurate results. A cosine distribution data file was computed and used to verify that **psens** would compute a value of 1.0. The image created from this dataset represents a perfect cosine-corrected photosensor (see Figure 7). If the input image is of sufficient resolution (at least 200 by 200 pixels), the pixel area weighting factors do not show appreciable error.

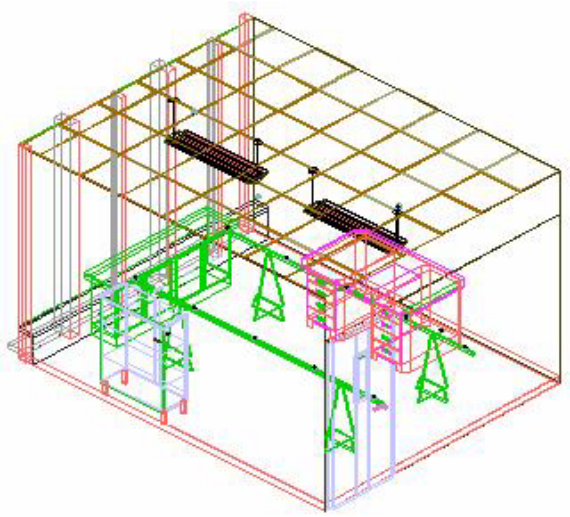

Figure 8. Wire-line image showing AutoCAD™ 3-D model of the Oakland Federal Building testbed office used for experimental validation of the simulation method.

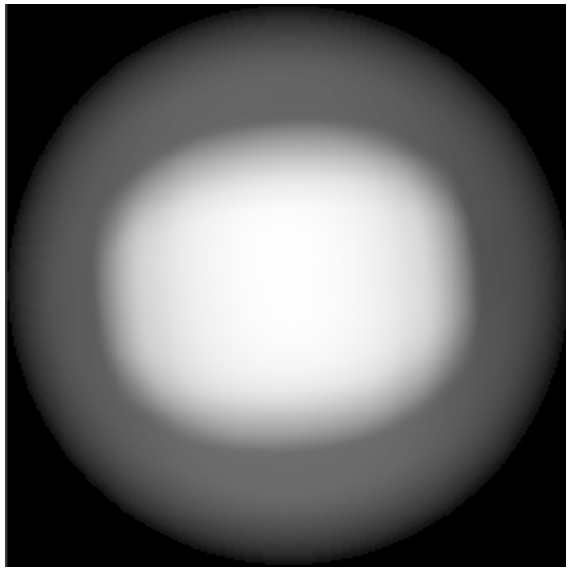

Figure 9. Spatial distribution fisheye image of the photosensor used in the Oakland Federal Building testbed.

Validation with experimental data was based on data from the Oakland Federal Building (OFB). The OFB testbed, located in Oakland, California (37°4' N, 112°1' W), is a pair of furnished office spaces outfitted with photosensor-controlled lighting systems, task photosensors, and data collection equipment. The rooms are 3.7 meters wide by 4.57 meters long by 2.68 meters tall (12 by 15 by 8.8 feet). Figure 8 shows a wire-line representation of

the office configuration, and Figure 4 shows a fisheye view. The room faces 63 degrees east of south and is glazed with 75-percent transmittance, floor-to-ceiling, single-paned windows. Room surface reflectances are 23 percent floor, 81 percent walls and 84 percent ceiling. The room is furnished with a large desk and two bookshelves with reflectances of 18 percent and 12 percent, respectively.

Table 1. Sensor voltage and workplane illuminance for three daytime and one nighttime measurement at the Oakland Federal Building testbed.

Daylight only				
Date	**Time**	**Volts**	**Lux**	**Lux/ Volt**
March 18	3:00 PM	2.61	645	247
April 16	3:00 PM	2.95	733	248
May 17	3:00 PM	3.36	797	237
			Avg.	**244**
Electric light only				
		1.00	585	585
Average task-sensor ratio for daylight				244
Task-sensor ratio for electric light				585
Task-sensor electric/daylight ratio				**2.39**

The lighting system consists of two four-lamp, 32-watt, pendant-mounted, direct-indirect luminaires with dimmable electronic ballasts. The photosensor is mounted near the center of the room underneath the luminaires and is pointed directly downward. The sensitivity distribution of the photosensor matches the distribution of sensor number eight (see Figure 9) described in the Bierman and Conway study. The data include interior workplane illuminance and photosensor signal strength taken every five minutes. The data were analyzed to find three spring days on which exterior illuminance remained fairly constant, indicating that there was no cloud cover, and during which the lighting system was completely dimmed (0.0 percent) because daylighting was sufficient. Clear days were selected to avoid introducing arbitrary error into the validation exercise with the complexities of the interaction of direct beam sunlight with fenestration apertures. March 18, 3:00 PM, April 16, 3:00 PM and May 17, 3:00 PM were selected. Photosensor signal strength in volts and workplane illuminance in lux were recovered from the data set and averaged from these three days when the lights were off. In addition, we collected data from a nighttime condition with lights at 100 percent power. We computed lux per volt for each of these days and then computed the average of these three days to minimize error resulting from changing sky conditions.

The ratio of task illuminance to photosensor signal voltage (task-sensor ratio) was selected as the basic measure of photosensor performance [Rubinstein, 1989]. The goal of the validation exercise was to compare the measured and simulated values for the task-sensor ratio for daylight only and electric light only conditions. A *Radiance* simulation of these same conditions was computed using the CIE clear sky model (`gensky`); the resulting fisheye images were processed with the **psens** program. We also attempted to validate the absolute light levels by computing fisheye images at the workplane and at the photosensor multiplied by the ideal cosine sensitivity distribution to compare the task and photosensor illuminance levels in *Radiance* with the nighttime measured conditions. As shown in Table 2, agreement for the electric lighting condition task-sensor ratio is quite strong with error of only 1.4 percent. The daylight condition also shows good agreement in the task-sensor ratio; this agreement could probably be improved if the Perez sky model [Perez, et al., 1993] were used instead.

Table 2. Validation results

Description	**Measured**	**Simulated**	**Error**
Daylighting task-sensor ratio	2.39	2.55	+6.7 %
Electric lighting task illuminance	485.0 lux	453.64 lux	-6.5%
Electric lighting sensor illuminance	94.0 lux	89.02 lux	-5.3%
Electric lighting task-sensor ratio	5.16	5.09	-1.4%

CONCLUSIONS

The availability of ray-tracing-based lighting simulation software (e.g., *Radiance*) and measured data for the angular and spectral sensitivity of photosensors makes it possible to effectively simulate the operation of photosensor-based electric lighting controls. The specific method described in this paper computes the signal of a photosensor by integrating the luminance of the surrounding interior and exterior surfaces and adjusting for the sensor's angular and spectral response. This integration is the equivalent of multiplying two fisheye images, one representing the angular sensitivity of the photo sensor and the other the scene luminance as seen by the sensor and summing the resulting pixel values.

This new method appears to accurately model and predict the response of photosensors. It was validated through comparison with measured data collected in an office space equipped with a photosensor-based electric lighting control system and separate task sensors for measuring workplane

illuminance. The implementation of the method is based on the *Radiance* lighting simulation and rendering software. At this point, the method is aimed mostly at manufacturers of photosensor controls to help with product design and to optimize control algorithms. The method is most appropriate for the design of specific applications of photosensor-based controls as well as for their calibration by allowing virtual operation, in a CAD model of the space where the sensors will be used, for multiple days and times during a year. The method can handle arbitrarily complex geometric configurations and complex fenestration such as venetian blinds. It provides immediate feedback in the form of a fisheye image of the photosensor angular sensitivity orientation. This method makes few assumptions, is highly accurate, and considers the effect of surface reflectance, geometric configurations, exterior shading, photosensor placement, and photometric calibration filters.

The method is limited by the lack of angular sensitivity information, which manufactures do not supply for their products. It is hoped that publications such as *Specifier Reports* [NLPI, 1988] will include these data in the future. The system has been validated only in a commercial office setting with horizontal glazing, but it is applicable to other building types and glazing systems.

Future plans are to include the new method in *Desktop Radiance* [LBNL, 2000], a Windows™ version of *Radiance* that has links to *AutoCAD*, which will make the program easier and faster to use. Integration of the new method in *Desktop Radiance* will allow architects and lighting designers to effectively evaluate alternative lighting control designs.

ACKNOWLEDGMENTS

This research effort was funded by the Pacific Gas & Electric Company (PG&E) through the California Institute for Energy Efficiency (CIEE), a research unit of the University of California. Publication of research results does not imply CIEE endorsement of or agreement with these findings, nor does it indicate the endorsement or agreement of any CIEE sponsor. Pacific Gas & Electric Company's funding is provided by California utility customers under the auspices of the California Public Utilities Commission. This work was also supported by the U.S. Department of Energy under Contract No. DE-AC03-7SF00098.

The authors give special thanks to Richard Mistrick and Francis Rubinstein for their valuable feedback during the refinement of the simulation technique, to Pacific Gas and Electric for providing the photosensor acceptance data and to Eleanor Lee for providing the Oakland Federal Building data.

REFERENCES

Bierman, A and Conway, K. 2000. Characterizing Daylight Photosensor System Performance to Help Overcome Market Barriers. *Journal of the IESNA* Vol. 29(no. 1): 101-115.

Chen, C. 1999. An Analysis of Automated Daylighting Dimming System Performance Under Optimal Calibration Conditions, A Thesis in Architectural Engineering. Penn State University, Department of Architectural Engineering.

Choi, A and Mistrick, R. 1997. On the Prediction of Energy Savings for a Daylight Dimming System. *Journal of the IESNA* Vol 26(no. 2) 77-90.

Clark, J and Janak, M. 1998. Simulating the Thermal Effects of Daylight-controlled Lighting. Building Performance Vol. 1:21-23.

Khodulev, A., Kopylov, E. 1996 Physically Accurate Lighting Simulation in Computer Graphics Software. Keldysh Institute of Applied Mathematics, Russian Academy of Sciences. Moscow State University. Moscow.

LBNL. 2000. The Desktop Radiance web site is: `http://radsite.lbl.gov/deskrad`

Lee, Eleanor, DiBartolomeo, D., Selkowitz, S. 1998. "Thermal and daylighting performance of an automated venetian blind and lighting system in a full-scale private office." *Energy and Buildings*. August: 47-63.

Love, J. 1995. "Field Performance of Daylighting Systems with Photoelectric Controls, " Presented at *3rd European Conference on Energy-Efficient Lighting*, Newcastle-upon-Tyne, UK.

Mardaljevic, J. 1995. Validation of a lighting simulation program under real sky conditions Lighting Res. Technology. 27(4) 181-188.

Mistrick, R., Chen, C., Bierman, A., and Felts, D. 2000. "A Comparison of Photosensor-Controlled Electronic Dimming Systems in a Small Office." *Journal of the IESNA* Vol. 28(no. 1): 59-73.

Mistrick, R. and Thongtipaya, J. 1997. "Analysis of Daylight Photocell Placement and View in a Small Office" *Journal of the IESNA* Vol. 26(no. 2):150-160.

National Lighting Product Information Program. 1988. *Specifier Reports: Photosensors*. Vol. 6; no. 1, Troy, NY: Lighting Research Center, Rensselaer Polytechnic Institute.

Perez, R., R. Seals, and R. J. Michalsky. 1993. All-Weather Model for Sky Luminance Distribution, Preliminary Configuration and Validation. Solar Energy, 50(3), 235-45.

Rubinstein, F. 1984. Photoelectric Control of Equi-ilumination Lighting Systems. *Energy and Buildings* Vol.6(1084): 141-150.

Rubinstein, F., Ward, G., and Verderber, R. 1989. "Improving the Performance of Photo-Electrically Controlled Lighting Systems," *Journal of the IESNA*, Vol. 18(no. 1): 70-94.

Ward, G. and Shakespeare, R. 1999. *Rendering With Radiance.* Morgan Kaufman. San Francisco.

Winkelmann, F.C., 1983. *Daylighting Calculations in DOE-2.* LBL-11353. Lawrence Berkeley National Laboratory.